remote sensing

MDPI

Article

Analysis and Comprehensive Evaluation of Urban Green Space Information Based on Gaofen 7: Considering Beijing's Fifth Ring Area as an Example

Bin Li [1,2,†], Xiaotian Xu [1,2,†], Hongyu Wang [1,2,3], Yingrui Duan [1,2,3], Hongjuan Lei [1,2,3], Chenchen Liu [1,2,3], Na Zhao [1,2], Xu Liu [4], Shaoning Li [1,2,3] and Shaowei Lu [1,2,3,*]

[1] Institute of Forestry and Pomology, Beijing Academy of Agriculture and Forestry Sciences, Beijing 100093, China; bjfulb@bjfu.edu.cn (B.L.); xuxiaotian@baafs.net.cn (X.X.); wanghongyu2023@163.com (H.W.); 18240453757@163.com (Y.D.); 18392712311@163.com (H.L.); chen2595832127@163.com (C.L.); zhaona@baafs.net.cn (N.Z.); lishaoning@baafs.net.cn (S.L.)
[2] Beijing Yanshan Forest Ecosystem Research Station, National Forest and Grassland Administration, Beijing 100093, China
[3] College of Forestry, Shenyang Agricultural University, Shenyang 110866, China
[4] Remote Sensing Application Center, China Academy of Urban Planning & Design, Beijing 100835, China; liuxu_ch@pku.edu.cn
* Correspondence: lushaowei@baafs.net.cn; Tel.: +86-010-62859212
† These authors contributed equally to this work.

Abstract: Urban green spaces constitute a vital component of the ecosystem. This study focused on urban green spaces located within the Fifth Ring Road of Beijing, using Gaofen 7 (GF-7) as the primary data source for analysis. The main objective was to develop a system for extracting and classifying urban green spaces in Beijing by applying deep learning and machine learning algorithms, and further, the results were validated with ground survey samples. This study provides detailed extraction and classification of urban green space coverage by creating a comprehensive evaluation system. The primary findings indicate that the deep learning algorithm enhances the precision of green space information extraction by 10.68% compared to conventional machine learning techniques, effectively suppresses "pretzel noise", and eventually aids in extracting green space information with complete edges. The thorough assessment of green spaces within the study area indicated favorable outcomes showing the high service capacity of park green spaces. The overall classification accuracy of the final extraction results was 94.31%. Nonetheless, challenges, such as unequal distribution of green zones and a significant fragmentation level throughout the study area, were still encountered. Consequently, the use of GF-7 high-resolution imagery, in conjunction with the collaborative application of deep learning and machine learning techniques, enabled the acquisition of highly accurate information regarding urban green zone coverage. According to the established grading standards of evaluation indices, the landscape pattern of urban green spaces within the study area was comprehensively assessed. This evaluation offers essential data support for monitoring urban green spaces and planning landscape patterns, thereby contributing to the achievement of sustainable development objectives related to urban greening and ecological conservation.

Keywords: urban green space; high-resolution remote sensing; machine learning; green space information analysis; evaluation system

check for updates

Citation: Li, B.; Xu, X.; Wang, H.; Duan, Y.; Lei, H.; Liu, C.; Zhao, N.; Liu, X.; Li, S.; Lu, S. Analysis and Comprehensive Evaluation of Urban Green Space Information Based on Gaofen 7: Considering Beijing's Fifth Ring Area as an Example. *Remote Sens.* **2024**, *16*, 3946. https://doi.org/10.3390/rs16213946

Academic Editor: Ashraf Dewan

Received: 6 September 2024
Revised: 20 October 2024
Accepted: 21 October 2024
Published: 23 October 2024

Copyright: © 2024 by the authors. Licensee MDPI, Basel, Switzerland. This article is an open access article distributed under the terms and conditions of the Creative Commons Attribution (CC BY) license (https://creativecommons.org/licenses/by/4.0/).

1. Introduction

Urban green spaces constitute a vital component of the urban ecosystem, significantly enhancing the urban ecological environment [1,2]. They are crucial in sustaining the equilibrium of carbon absorption and emissions within the ecosystem [3], thus improving the local climate of urban areas, fostering the green development of cities, and contributing

to the overall well-being of residents [4–6]. Urban parks, as a quintessential type of green space in cities, offer significant ecological services to the public.

Landscaping plays an indispensable role in cities, and the Evaluation Standard for Urban Landscaping (GB/T50563-2010) [7] is the only standard among the existing standards in China that aids in the systematic evaluation of urban landscaping. It represents sufficient time for understanding construction, management, and benefits of landscaping [8]. In recent years, China has increased its research efforts in the field of urban landscaping and greening construction. Moreover, on a yearly basis, the country conducts a physical examination of urban parks in the national ecological garden city, as well as performing other assessments, thus paying more attention to the enhancement of the city's ecological function, a comprehensive level of urban construction and management, and the level of urban services for the people. This makes it crucial for advancing scientific urban planning and management to establish standardized protocols for the survey and assessment of the existing conditions of urban landscaping. Thus, it is required to develop a precise and effective evaluation methodology capable of facilitating the real-time monitoring of urban green space information and assessing its ecological functions, all while minimizing manual labor requirements [9–11].

Urban green spaces exhibit a scattered distribution, characterized by diversity and significant heterogeneity. Consequently, compared to medium- and low-resolution remote sensing imagery, submeter resolution remote sensing imagery can more accurately and quantitatively reflect the spatial distribution pattern of green space, and it can better reveal its impact on ecological functions [6,10]. The effective execution of "High-Resolution Earth Observation System of Systems" and the rapid development of high-resolution space probe technology have provided important data support for the more accurate real-time monitoring of urban features [11]. Concurrently, the ongoing advancements in deep learning technology, coupled with the introduction of novel algorithms, can significantly enhance the precision and efficacy of remote sensing monitoring, facilitating the promotion of urban three-dimensional digital construction and the development and rationalization of resource use [12,13]. In contrast to conventional machine learning techniques, deep learning methodologies can more comprehensively analyze the spectral, textural, and potential feature information inherent in extensive datasets while also facilitating automatic feature selection and extraction, which has led to the high accuracy of deep learning methods in image classification and recognition [14]. Recently, deep learning has emerged as a significantly important methodological approach for the extraction of feature information. Deep learning-based methodologies for remote sensing image classification have been employed in the extraction of building features [15,16], road extraction [17], land classification [18,19], and crop categorization [20], and significant progress has also been made in the area of urban green spaces [13,20]. In the field of urban green space classification via remote sensing images, Helber et al. [18] used the FCN-8s model to extract street-view green and blue spaces from the Tencent map and street-view data, and further determined the relationship between green and blue space of street-view images and depression in the elderly. Vigneshwaran and Vasantha considered that irrespective of the method used, the precision of green space classification in high-spatial-resolution images was the highest, and the deep learning method showed superior performance compared to traditional methods [19]. Martins et al. used various CNN architectures (Ostu, Meanshift, FNEA, and two Deeplabv3+variants), and classified five tree species in tropical urban environments by using aerial photographs with an accuracy of 86% [20]. Currently, deep learning and machine learning methods still bring forward some problems in the classification research on urban green space. For example, in the Evaluation Standard for Urban Landscaping (GB/T50563-2010), the traditional per capita green space area, green coverage rate, urban green space rate, and other indicators exhibit difficulties in describing the layout of urban park green space at a spatial resolution. There are few correlation analyses of the basic characteristics of green space and the landscape pattern index of all parks in a region, and the scope of previous studies is small. It is difficult to distinguish small patches or

complex plant communities. With the rapid renewal of the city, numerous small green spaces with blurred boundaries and inaccurate information occur inside a park, which impedes the acquisition and research on green space information. As an important index of park environmental quality, blue and green space and the landscape pattern index can provide a reference for the construction of urban green space and living environments.

Against this background, numerous studies on urban parks have emerged [21–24]. Previous studies mostly used satellite images such as TM/ETM + as a data source [25] and focused on the evaluation of green landscape quality and ecological service value using a single index, such as blue–green space and landscape patterns of single or several parks [26–30].

In the new round of the Beijing Master Plan, Beijing is positioned as a "Livable City", which shows the great importance attached to the urban ecological environment and the urgent demand for green space [31]. To promote the "new urbanization with people as the core" and "comprehensive improvement in the quality of cities", and to adapt to the new requirements of China's economic and social development on urban landscaping [32–36], this study tried to expand some of the evaluation indices of the Evaluation Standard for Urban Landscaping (GB/T 50563-2010) and lay the foundation for the construction of a new evaluation system for urban landscaping [34–37]. Consequently, to investigate the application prospects of high-resolution remote sensing imagery, the establishment of a comprehensive evaluation system for the landscape pattern of urban gardening and greening is important for gardening and greening initiatives in Beijing as it enters a new phase of development [38–41].

This study focuses on the urban green spaces located within the Fifth Ring Road of Beijing. In contrast to the traditional machine learning methods, herein, high-submeter-resolution remote sensing data were applied, along with deep learning and machine learning models, to extract and analyze green space information within the designated area. Further, relevant field surveys, the spectrum, the texture, and the potential feature information of a large amount of data were also combined, and automatic feature selection and feature extraction as well as information regarding roadways and residential areas were used. This allowed us to screen and classify parklands and to develop a comprehensive information evaluation system for urban green zones, aiming at assessing the evaluation grade of the comprehensive service capacity of urban green spaces within the designated study area and to explore the following issues: (1) the viability and precision of deep learning technology in the extraction and classification of urban green zone information; (2) the comprehensive evaluation grading standard for urban green space information in the study area from the three aspects of basic quantitative characteristics, green space landscape pattern, and park green space service capacity; and (3) the spatial configuration of various urban green spaces, along with recommendations for enhancing the ecological functionality of these areas. This study serves as a reference for the development and administration of sustainable, ecologically friendly urban environments.

2. Materials and Methods

2.1. Study Area

As the capital of China, Beijing is a central hub for political, cultural, international, and scientific and technological activities. Geographically, it is situated between longitudes 115.41° and 117.51° east and latitudes 39.44° and 41.05° north. The city is located in the northern part of China, characterized by a topography that gradually descends from the west to the southeast. Green spaces are strung together into a combination of points, lines, surfaces, belts, and rings through green corridors, constituting the characteristics of urban greening in Beijing [22]. The study area, the Fifth Ring Road of Beijing, covers 666 km^2. Figure 1 presents a false-color GF-7 image of the research area, which was obtained using the near-infrared, blue, and green bands.

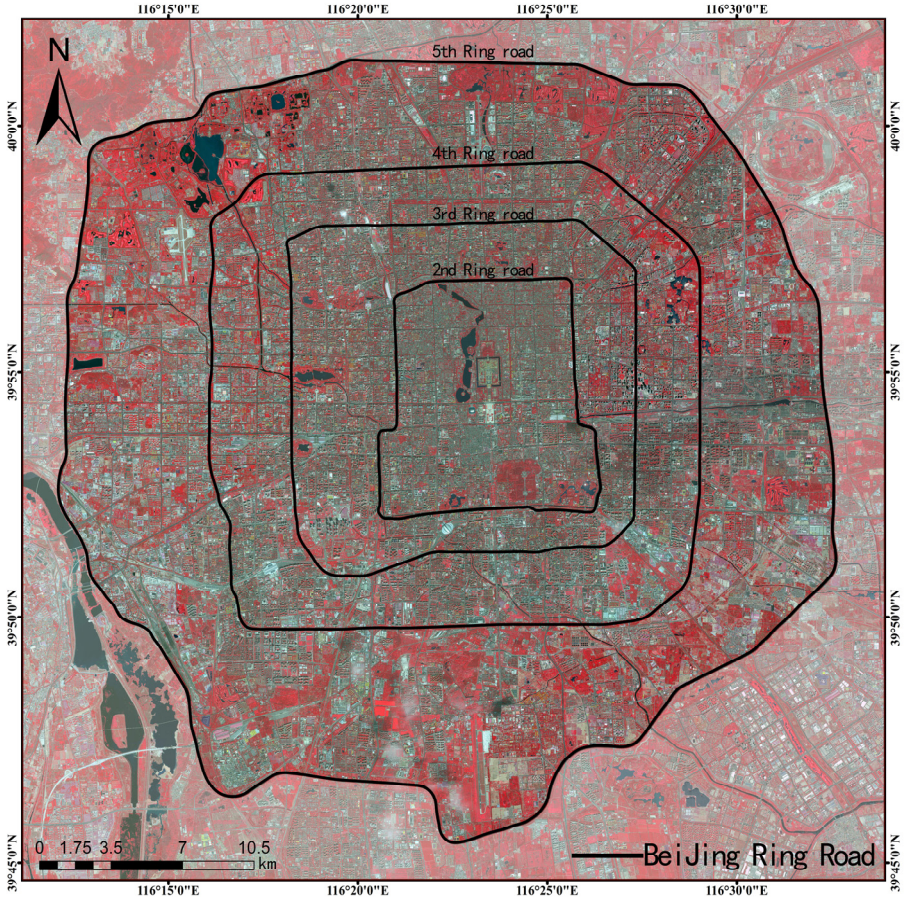


Figure 1. False-color GF-7 image of the study area.

2.2. Data Sources

2.2.1. Satellite Image Data

In this study, remote sensing imagery obtained from the GF-7 satellite, a Chinese satellite, was used as the primary data source. The panchromatic stereoscopic image pair has a resolution of 0.8 m, whereas the multispectral image has a resolution of 3.2 m. The imagery was acquired from the terrestrial observation satellite service network (https://data.cresda.cn (accessed on 1 November 2021)). Considering the climate-based vegetation characteristics, image data should be collected during the vegetation growth period to obtain more accurate results. This research primarily used four GF-7 remote sensing image datasets collected between 15 April and 15 October 2021. The data processing procedure encompassed several stages, including orthographic correction, atmospheric correction, geometric correction, fusion, and mosaic processing. Following the resampling phase, images with submeter precision and a four-band resolution of 0.6 m were produced.

2.2.2. Supporting Data

Auxiliary data pertaining to road infrastructure and residential areas within the study region were gathered, and the coordinate system was standardized. The road data for Beijing were obtained from Open Street Map (https://openstreetmap.org (accessed on 15 March 2022)), and the information regarding residential areas and park locations was obtained from the Amap Open Platform Web API service (https://lbs.amap.com (accessed on 20 March 2022)). The Display XY Data tool in ArcGIS 10.7 was employed to transform the field survey sample points into vector point data to assess the precision of the classification of urban green zones (see attached Schedule S1).

2.3. Green Space Classification and Extraction System (U-net-SVM)

Herein, a hybrid approach, integrating both deep learning and machine learning models, was employed to develop a system for the extraction and classification of urban green zones. By combining the analytic hierarchy process and the expert scoring method, the weights of the criterion layer and each index layer were determined. Owing to different units and dimensions used for each indicator, the data could not be directly compared. Therefore, when conducting a multi-index comprehensive evaluation, all indicators were standardized. Consequently, the urban green space information was subjected to a thorough evaluation and analysis via the evaluation index system developed in this study (see Figure 2).

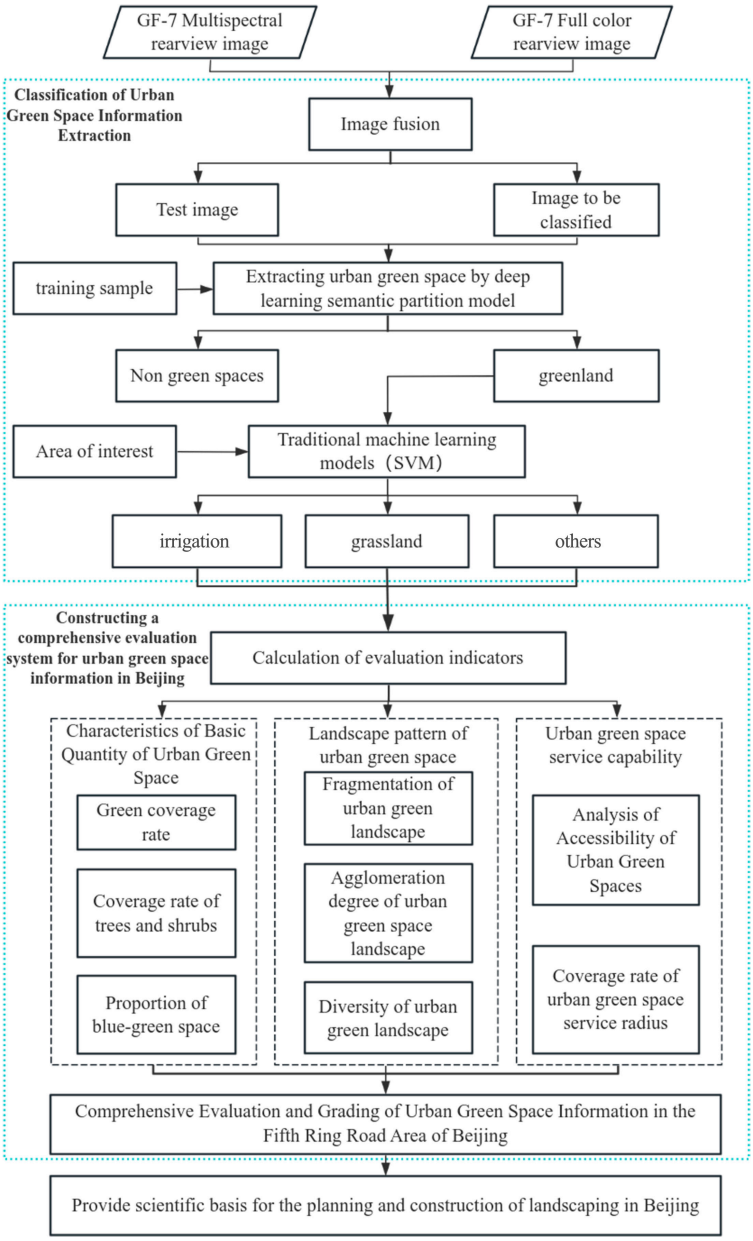


Figure 2. Flowchart of the method.

2.3.1. Information Extraction on Urban Green Spaces

(1) Deep learning model construction

In this study, a deep learning model was employed to assess the comprehensive coverage of green spaces within the study area. U-Net models usually use a variety of

indicators in the evaluation, which can be used to comprehensively assess the model performance. In particular, in the image segmentation task, IoU is an important evaluation index that represents the ratio between the intersection of the model prediction result and the real label; the larger the IoU, the better the segmentation effect of the model. In this study, the U-Net architecture, which demonstrates consistent classification performance, was selected as the deep learning classifier [42,43]. It refers to a fully convolutional neural network that operates in an end-to-end manner, is distinguished by the exclusive use of convolutional layers, devoid of any fully connected layers, and can handle input images of different sizes. The encoder uses a common convolutional neural network structure containing a convolutional layer and a maximum pooling layer for down-sampling. Shallow down-sampling captures some simple information about the image, such as boundaries and colors; as the sensory field becomes larger and undergoes more convolutional operations, the deeper structure captures the abstract features of the image.

(2) Production of a training sample set for Beijing urban green space extraction

Notably, green plants have high reflectivity in the near-infrared band; therefore, the spectral information of the GF-7 remote sensing data can be used as the classification feature to continuously label green and non-green spaces to construct training samples. By simulating standard false-color images, RGB was synthesized for display in the near-infrared, red, and green light bands. By integrating field survey with high-resolution remote sensing imagery, the outcomes of visual interpretation could be refined, leading to the generation of a more precise labeled image [5,13,18,38,44,45].

Deep learning algorithms are difficult to be trained directly on high-resolution large-format images and labeled images. Therefore, in this study, a regular grid cropping method was adopted to crop the images and corresponding labeled images of the two test sample areas with image blocks measuring 256 × 256 in size (see Figure 3). Cropping must ensure that the numbering of the small images obtained by cropping is consistent with that of the corresponding labeled images; in total, 2450 images and corresponding labeled images were obtained by cropping. Subsequently, the green space sample dataset was augmented through horizontal, vertical, and diagonal flipping. After processing, the number of training and validation sets was expanded to 7350.

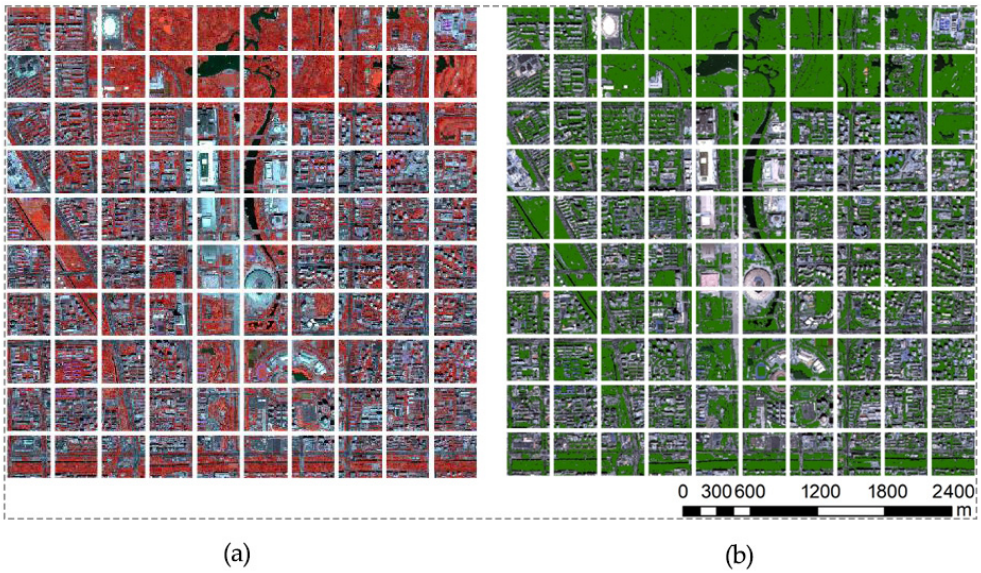


Figure 3. Schematic illustration of regular grid clipping for RS imagery and label image: (**a**) RS imagery of the test areal (the red areas indicate vegetation with the highest reflectance in the near-infrared band); (**b**) corresponding truth label data (the green areas indicate the true vegetation after annotation).

(3) Deep Learning Model Training and Prediction

By using the urban green space extraction training sample dataset, the preliminary urban green space extraction model was developed through the training of the U-Net model. During the training process, network parameters, including batch size and learning rate, were systematically modified to increase the classification accuracy. The quantity of categories was established at 2, with a total of 20,000 iterations, a batch size of 10, and a fundamental learning rate of 1×10^{-3}. After several training iterations, the validation data were enhanced, the number was expanded to 3 times the original, and the training model was completed.

2.3.2. Classification of Urban Green Zone Information

Urban green zones can be divided into irrigation (composed of trees and shrubs) and grass, according to their types. Owing to the complexity of urban green space classification, the classification and extraction of irrigation and grass cannot be realized only by the spectral features of the images. Therefore, in this study, based on U-net to extract green zone information, the supervised classification method of traditional machine learning was employed, using GF-7 remote sensing image synthesis as the standard false color. According to the vegetation spectrum and texture decoding characteristics, the green space information in the image of the sample collection area was discreetly labeled into two types, namely irrigation and grassland, through artificial visual interpretation. In the standard false color composite images, the texture features of the irrigation areas appear coarser, while those of the grassland areas appear finer; the irrigation areas are depicted in red and dark red, whereas the grassland areas are shown in light red. The irrigation areas are mainly distributed within parks, residential areas, and along roadsides; the grassland areas are primarily found in parks, squares, and golf courses. The training sample was selected by drawing a polygon interest area. The separability between each sample type was represented by the Jeffries–Matusita distance and conversion separability parameters, and the combinations of areas of interest were listed from small to large, according to the size of the separability values. The values of these two parameters ranged from 0 to 2.0, and in general, a sample separability >1.8 was considered satisfactory, with greater separability indicating better separability. The separation degree between the collection of irrigation and grass samples was 1.81, indicating the qualification of the sample selection. The support vector machine (SVM), with a high classification accuracy, a better classification effect, and a capability to extract the target features more accurately, was used as a classifier [18].

2.3.3. Analysis of Urban Green Zone Information

Using the outcomes of green zone extraction in conjunction with point of interest (POI) data related to parks, as well as road network data, the information pertaining to park green spaces was systematically extracted. The spatial location information of green zones within parks in the study area was determined through an analysis of park point density and the standard ellipse difference. Subsequently, the distribution model for parklands was computed by the average nearest proximity method.

2.3.4. Accuracy Verification

To assess the validity of the extraction outcomes produced by the classification system (U-net-SVM) developed in this study, a comparative analysis was conducted between these results and those obtained solely through the SVM methodology. The prediction outcomes for urban green space derived from both approaches, along with the corresponding ground truth data, were compared by using a confusion matrix. Overall, 262,518 pixels were randomly selected from 100 sample areas representing true values of shrub, grassland, and non-green space. The metrics of user's accuracy (UA), producer's Accuracy (PA), overall accuracy (OA), and kappa coefficient were computed through the application of a confusion matrix. Table 1 presents the calculation equations.

Table 1. Index calculation equations.

Evaluation Indicators	Equation
UA	$UA = \frac{TP}{TP+FP}$
PA	$PA = \frac{TP}{TP+FN}$
OA	$OA = \sum_{i=1}^{n} \frac{X_{ii}}{N}$
Kappa	$K = \frac{N\sum_{i=1}^{n} X_{ii} - \sum_{i=1}^{n}(X_{i+} \times X_{+i})}{N^2 - \sum_{i=1}^{n}(X_{i+} \times X_{+i})}$

Note: N is the composite of the number of categories (total number of pixels); n is the category. X_{ii} denotes the diagonal element of the confusion matrix, i.e., the number of pixels for category i; X_{i+} represents the aggregate of the column values within the category; and X_{+i} denotes the total of the row values within the same category.

2.4. Urban Green Space Information Evaluation Index System

2.4.1. Analysis and Calculation Methods of Urban Green Zone Information

The study area encompasses a significant number of parks, and the spatial distribution patterns of these parks vary between the inner (2nd Ring Road) and the outer rings. In this study, park green space information was analyzed from three aspects, namely, basic quantity characteristics, green space landscape pattern, and service capacity.

(1) The analysis of the characteristics of the basic quantity of urban green zones included the green coverage rate, the irrigation coverage rate, and the ratio of blue to green space, which characterizes the situation of the basic quantity of urban green zones. The corresponding equations are as follows:

$$\text{Green coverage}(\%) = \frac{\text{Vertical projection area of all vegetation within the park}\left(\text{hm}^2\right)}{\text{Park area}\left(\text{hm}^2\right)}$$

$$\text{Percentage of irrigation cover}(\%) = \frac{\text{Vertical projection of irrigation in the park}\left(\text{hm}^2\right)}{\text{Vertical projection area of all vegetation within the park}\left(\text{hm}^2\right)}$$

$$\text{Percentage of blue} - \text{green space}(\%) = \frac{\text{Total area of green space and water within the park}\left(\text{hm}^2\right)}{\text{Park area}\left(\text{hm}^2\right)}$$

(2) The Fragstats software was employed to compute three indices pertaining to landscape fragmentation, landscape aggregation, and landscape diversity, (see Table 2 for further details). The Fragstats 4.2.1 software is a spatial pattern analysis program used to quantify landscape structure and mainly applied to calculate multiple landscape pattern indices of classified map patterns [25,46,47]. Data analysis and processing are implemented through a graphical user interface or a command line. Collectively, these indicators illustrate the configuration and distribution of urban green landscape patches.

Table 2. Equations for calculating the landscape pattern index.

Landscape Index Name		Unit	Index Meaning	Equation	Reference
Landscape fragmentation	Plaque density, PD	number·hm^{-2}	With increasing value, the fragmentation of landscape patches increases.	$PD = \frac{NP}{A}$	[25]
	Mean patch area, AREA_MN	hm^2	Characterizes the degree of landscape fragmentation.	$AREA_MN = \frac{A}{NP}$	
Landscape aggregation	Connectivity index, COHESION	%	Characterizes the degree of aggregation of homogeneous patches in the landscape.	$COHESION = \left[1 - \frac{\sum_{i=1}^{n} P_{ki}}{\sum_{i=1}^{n} P_{ki}\sqrt{a_{ki}}}\right]\left[1 - \frac{1}{\sqrt{A}}\right]^{-1}$	[26]
	Aggregation index, AI	%	Characterizes the degree of aggregation of homogeneous patches in the landscape.	$AI = \left[\sum_{i=1}^{n}\left(\frac{g_{ii}}{\max g_{ii}}\right)/pi\right]$	[27]

Table 2. *Cont.*

Landscape Index Name		Unit	Index Meaning	Equation	Reference
Landscape diversity	Shannon Diversity Index, SHDI	—	Reflects the heterogeneity and fragmentation of the landscape.	$SHDI = -\sum_{i=1}^{m}(p_i \ln p_i)$	[25]
	Shannon Even Index, SHEI	—	Reflects that the landscape is dominated by one or a few dominant tile types.	$SHEI = \frac{-\sum_{i=1}^{m} p_i \ln(p_i)}{\ln m}$	

Note: NP represents the aggregate quantity of landscape patches; A represents the cumulative area of landscape patches.; E is the sum of the boundaries of various types of patches in the landscape; n represents the aggregate quantity of plaques of a specific type.; p_{ki} is the plaque circumference; a_{ki} is the plaque area; and g_{ii} represents the ratio of the area occupied by an i-th patch type to the overall landscape area.

(3) In this study, the service capacity of urban green zones within the Fifth Ring Road area of Beijing was examined, focusing on the coverage rate of the service radius of these green spaces and their accessibility [1,48–50]. In accordance with the calculation criteria outlined in the National Garden City Selection Standards, a service radius of 500 m was designated for parks and green spaces exceeding 5000 m^2 in area, and a service radius of 300 m was assigned to those smaller than 5000 m^2. Table 3 presents the selection criteria for the coverage of the urban green zone service radius and the accessibility of urban green zones.

Table 3. Green space service radius coverage and green space accessibility.

	Percentage of Residential Land Area	Service Radius	Walking Time	Walking Distance
Garden City Selection Criteria	Less than 5000 m^2	300 m	5 min	420 m
	5000 m^2 and above	500 m	5–15 min	1250 m
			15–30 min	2500 m

2.4.2. Methods for Constructing Evaluation Index Systems

In this study, the analytic hierarchy process in conjunction with the expert scoring method was used to distribute an electronic questionnaire to 20 experts and scholars specializing in ecology, gardening, and planning. The significance of each indicator was evaluated and scored (Schedules S1 and S2) to ascertain the weights of the criterion layer as well as those of each index layer (Table 4). The analysis of weight values revealed that the service capacity of urban green spaces was prioritized over both the landscape pattern and the fundamental quantitative characteristics of these spaces [1,49]. This trend suggests that, in the development of urban green zones in China, an increasing emphasis is placed on the service capacity of such areas, followed by considerations of their landscape patterns [2,51]. Consequently, the significance of traditional quantitative metrics appears to be diminishing.

Table 4. Thorough assessment of the significance of each layer within the index.

Target Level	Standardized Level	Weight, W_i	Indicator Level	Weight, W_j
Beijing Urban Green Space Information Comprehensive Evaluation System, A	Evaluation of basic quantitative characteristics of cities, B1	0.27	Green coverage, C1	0.1188
			Percentage of irrigation cover, C2	0.0621
			Percentage of blue–green space, C3	0.0891
	Evaluation of urban green space landscape pattern, B2	0.36	Landscape fragmentation, C4	0.1620
			Landscape aggregation, C5	0.0972
			Landscape diversity, C6	0.1008
	Evaluation of the service capacity of urban green spaces, B3	0.37	Green belt service radius coverage, C7	0.2183
			Green space accessibility, C8	0.1517

3. Results

3.1. Comparison of Urban Green Zone Classification Results

The outcomes of the deep learning U-net model were evaluated and compared with those obtained from the SVM methodology. In the local extraction outcomes of the two

classification techniques, the green color denotes areas of irrigation, red signifies grassland, and the uncolored regions indicate non-green spaces (Figure 4). The blue and green spaces were extracted from the water body and the green space through the formula. The classification results indicate that the performance of the U-net-SVM surpasses that of the SVM in terms of extraction efficacy (Table 5). The edges of the greenery information extracted by the U-net-SVM by using the deep learning U-net model were more complete, and they could effectively separate the green from the non-green spaces and reduce the influence of other feature information. Herein, "green space" refers to all types of green spaces, such as trees, shrubs, and grass. The outcomes derived solely from the SVM exhibited a pronounced distortion, commonly referred to as "pretzelization". The shaded regions of the image were inaccurately categorized as urban green spaces, thereby compromising the overall accuracy of the classification and recognition processes. Grassland covers a small distribution area in the city and is easily covered by tall trees and buildings, indicating omissions in the extraction of grassland by both methods.

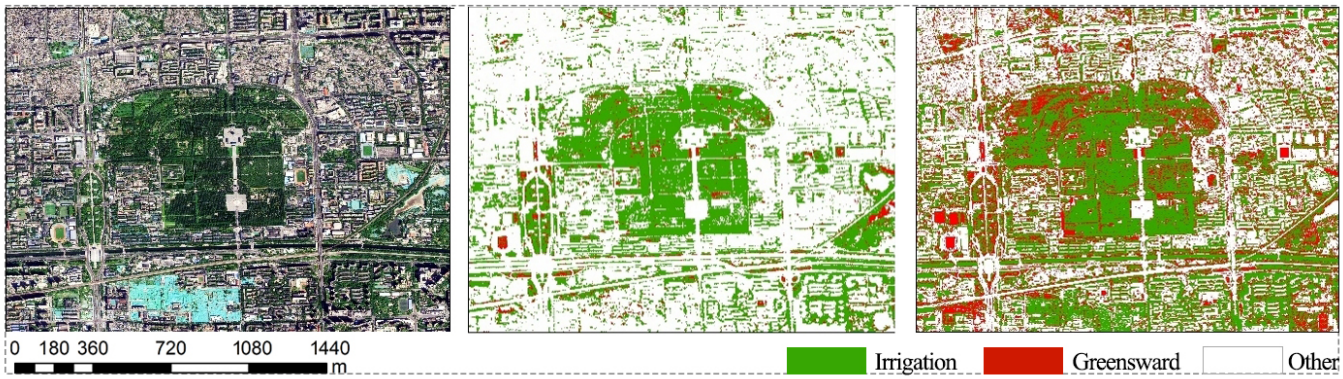


Figure 4. Comparison of the classification results between the classification system (U-net-SVM) and SVM method only: (**a**) localized images of the study area; (**b**) classification system (U-net-SVM) local area green space extraction results; (**c**) SVM local area green space extraction results.

Table 5. Comparison of the classification accuracies between the classification system (U-net-SVM) and the SVM method only.

Classification Method	Category	Producer Precision (%)	User Precision (%)	Overall Classification Accuracy (%)	Kappa Coefficient
U-net-SVM model	Irrigation	96.81	88.56	94.31	0.88
	Grassland	57.47	91.34		
	Non-green space	99.58	96.67		
SVM	Irrigation	85.07	75.32	83.63	0.71
	Grassland	99.05	51.89		
	Non-green space	80.61	99.99		

The findings derived from the confusion matrix indicate that the proposed classification system (U-net-SVM) demonstrates markedly superior accuracy compared to that of the SVM alone. Specifically, the overall classification accuracy improved by 10.68%, whereas the kappa coefficient increased by 0.17. The producer accuracy and the user accuracy of the non-green spaces were the highest, with values of 99.58% and 96.67%, respectively. The producer accuracy of the grassland was the lowest, at 57.47%, with a user accuracy of 91.34%. These findings indicate that the classification system (U-net-SVM) developed in this study for the extraction of urban green space information in Beijing could effectively retrieve such data.

3.2. Evaluation of the Results of Characterization of the Basic Quantity of Urban Green Spaces

3.2.1. Evaluation of the Basic Quantitative Characteristics of Urban Green Zones

The assessment of the fundamental quantitative characteristics within the five-ring framework yielded a score of 0.84, corresponding to an evaluation grade of I (Figure 5a). This indicates that the overall configuration of urban green zone distribution within Beijing's Fifth Ring Road is exemplary. The area designated for urban green zones is adequate, and the fundamental quantitative characteristics of the city are deemed reasonable, thereby facilitating the effective use of the functional value associated with urban green zones. The green space of Beijing's Fifth Ring shows an increasing trend, and the distribution of green space in parks shows a pattern of "more in the north and less in the south". Vegetation mainly occurs in large patches, distributed in the western and northern areas of the Fourth to the Fifth Ring Road. The assessment of the fundamental quantitative characteristics of urban green spaces located within the Fourth to the Fifth Ring yielded the highest evaluation results, classified at grade I. The evaluation grades of the Second Ring, the Second to Third Ring, and the Third to Fourth Ring were grade II. The assessment outcomes followed the order Second Ring, Second to Third Ring, Third to Fourth Ring, and Fourth to Fifth Ring. Furthermore, it is recommended that the area encompassed by three rings be suitably expanded.

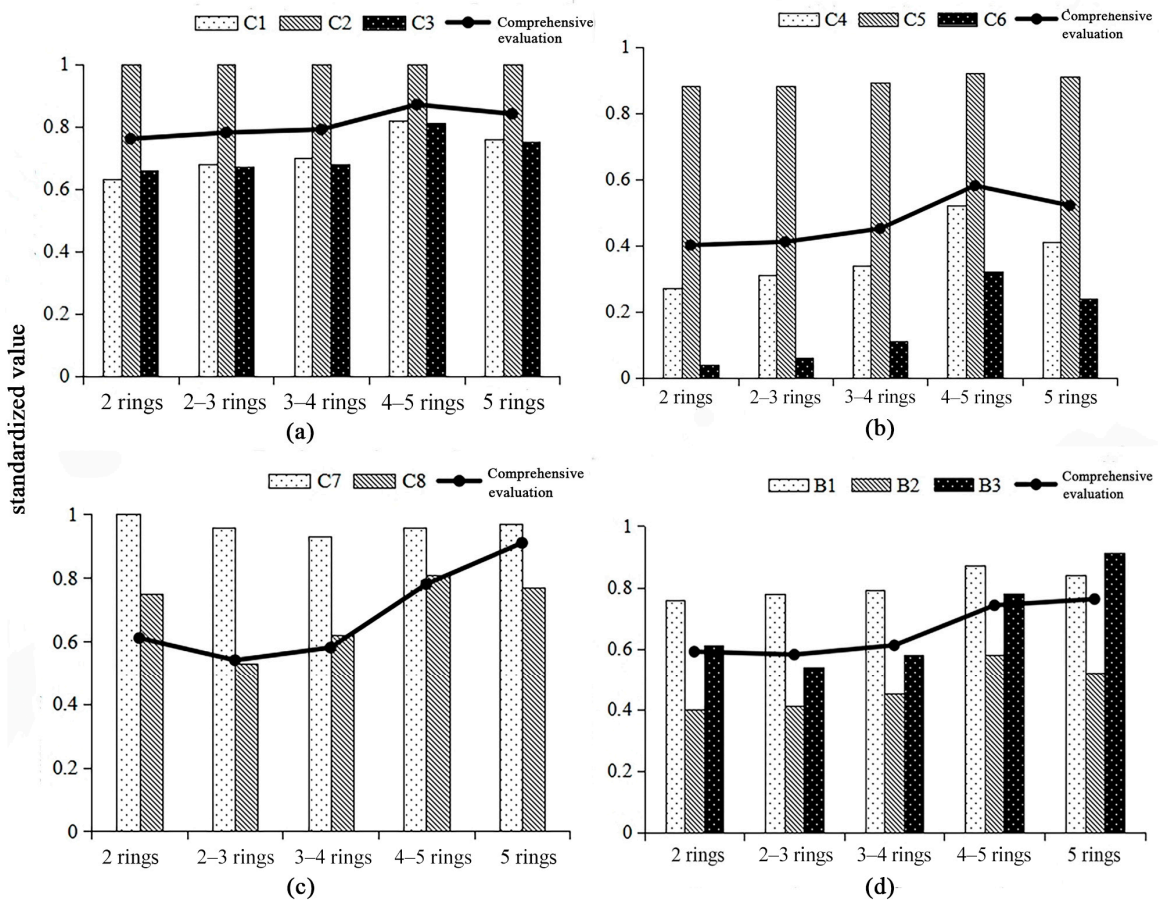


Figure 5. Comprehensive evaluation of indicators of the study area in different ring belts: (**a**) basic quantitative characteristics of urban green zones; (**b**) green space landscape pattern; (**c**) green space diversity; (**d**) information on urban green spaces.

The green zone coverage area of parks within the study area can reach more than 60% (Figure 6a). Based on the analysis results, the parks within the study area exhibit a substantial degree of green space coverage, regardless of their location in either the inner or outer ring road regions.

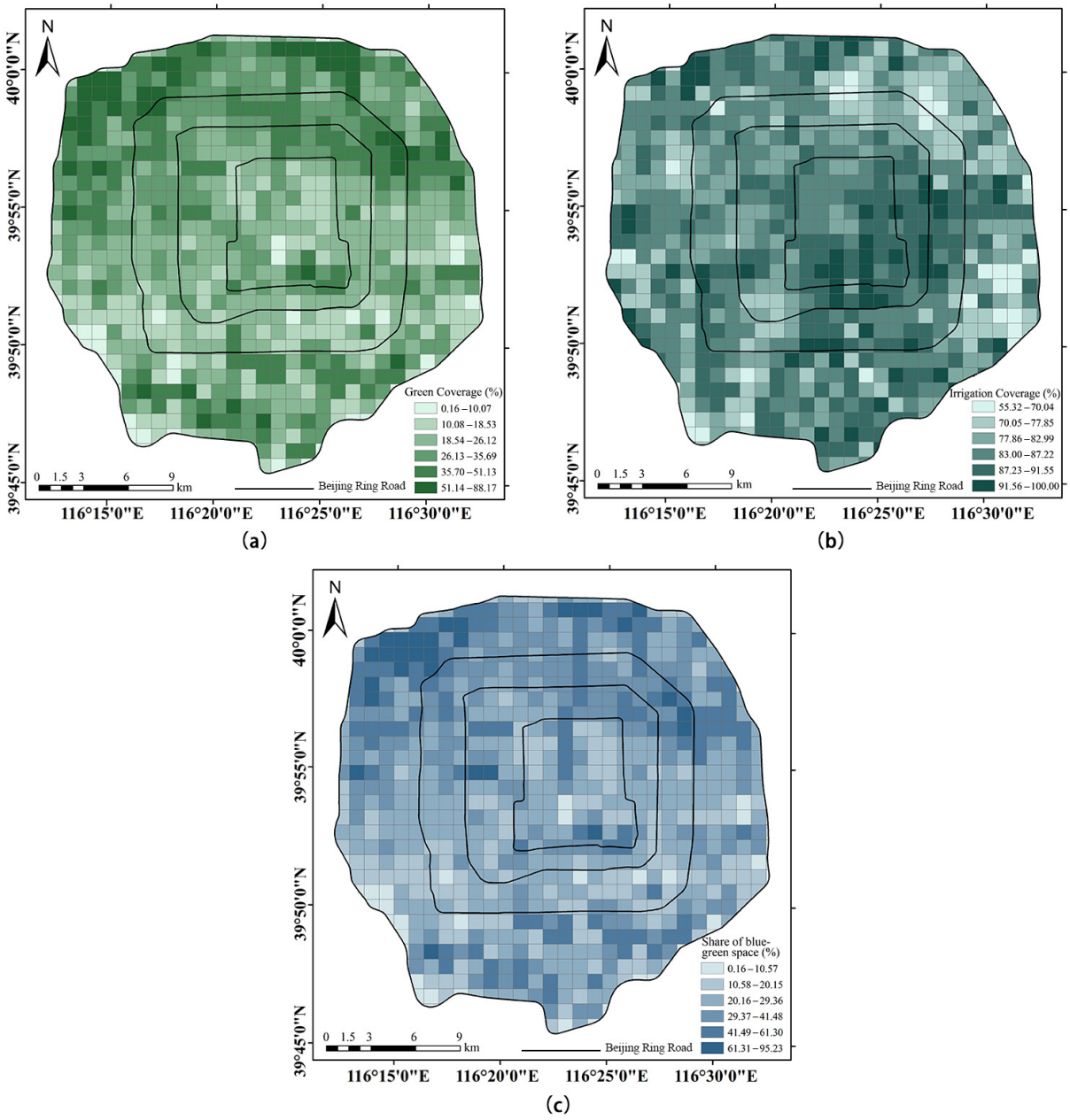


Figure 6. Spatial distribution maps of basic quantitative characteristics of urban green zones in the district: (**a**) spatial distribution of green coverage; (**b**) spatial distribution of irrigation cover; (**c**) spatial distribution of blue–green space share.

Regions exhibiting elevated levels of tree cover are predominantly located within the third ring, specifically in the southern section of Dongcheng District and the western area of Chaoyang District (Figure 6b). In the 1 × 1 km grid, the minimum value of green coverage of arborvitae within the fifth ring was 55.32%, the maximum value was 100%, the average value was 83.9%, and the percentage of grids with higher-than-average values was 56.43%. These findings indicate that irrigation holds a predominant role in the urban green spaces located within the confines of the study area, thereby influencing the overall green coverage metrics. Irrigation areas are primarily concentrated in the southeastern region of the Third Ring Road, which indicates homogeneity in vegetation types, characterized by a substantial prevalence of irrigation and a notable deficiency in grasslands. Furthermore, the coverage of irrigation in the northeastern, southeastern, and southwestern areas within the Fourth and Fifth Ring Road was comparatively low.

Areas with high amounts of blue–green spaces were mostly large park aggregation areas, and the largest range was distributed in the northwest of the fourth–fifth ring (Figure 6c). In the 1 × 1 km grid, the minimum value of the blue–green space proportion in the fifth ring was 0.16%, the maximum value was 95.23%, and the average value was 29.16%. The percentage of grids with higher-than-average values was 40.39%. These findings indicate that the spatial distribution of blue–green spaces within the study area closely resembles that of green coverage, predominantly concentrated in the northern region of the city. Furthermore, the allocation of parks significantly influenced the ratio of blue–green space across the entire area.

3.2.2. Normalization of the Basic Quantitative Characteristics of Urban Green Zones

According to the requirements outlined in the Selection Criteria for National Garden Cities in 2022, a green coverage rate of 41%, a coverage rate of irrigation of 60%, and a ratio of blue and green space of 43% were taken as standard values. The current status of the indicators was standardized according to the equation for the urban green coverage rate, and the scores of green space coverage within the study area were obtained (Table 6). The standardized metrics for the green coverage rate and blue–green space ratio within the study area, as well as across various ring zones of Beijing, consistently exceeded 0.6. Furthermore, the assessment classifications for these metrics attained a minimum of level II or higher. Among them, the standardized result of the fourth–fifth rings was the largest, and the standardized processing result of greening coverage was 0.82, with an evaluation grade of I. The standardized result of the blue–green space occupation ratio was 0.81, with an evaluation grade of I. The standardized value of arbor irrigation coverage within the Fifth Ring Road and different ring belts was 1, with the evaluation grade reaching I.

Table 6. Standardized basic quantitative features.

Indicator Layer	Study Area	Standard Value (%)	Standard Basis	Normalized Values	Evaluation Rating
Green coverage, C1	2 rings	41	Selection Criteria for National Garden Cities 2022	0.63	II
	2–3 rings			0.68	II
	3–4 rings			0.70	II
	4–5 rings			0.82	I
	5 rings			0.76	II
Irrigation coverage, C2	2 rings	60	Selection Criteria for National Garden Cities 2022	1	I
	2–3 rings			1	I
	3–4 rings			1	I
	4–5 rings			1	I
	5 rings			1	I
Proportion of blue–green space, C3	2 rings	43	Selection Criteria for National Garden Cities 2022	0.66	II
	2–3 rings			0.67	II
	3–4 rings			0.68	II
	4–5 rings			0.81	I
	5 rings			0.75	II

3.3. Analysis of Green Zone Landscape Pattern

3.3.1. Standardized Processing of Green Zone Landscape Pattern Analysis Results

The assessment of green space landscape fragmentation within the Fifth Ring Road of Beijing, as well as across various ring belts, indicates an overall evaluation grade of III. This result suggests a low to moderate degree of landscape fragmentation (Table 7). Noteworthily, within this context, only four–five rings of the green landscape exhibited a low level of fragmentation, as indicated by a standardized score of 0.52 and an assessment classification of III. The concentration degree of green zones in the Fifth Ring Road and in different ring belts was at the level of I, and the landscape concentration in the Fourth and Fifth Ring Road was the highest, with a standardized result of 0.92. The standardized result of landscape diversity in the five rings was 0.24, and the evaluation grade was IV. Only the green landscape diversity in the fourth and fifth rings in different rings could reach the IV level, and the other rings were all classified as grade V.

Table 7. Basic quantitative characteristics of urban green space within the Fifth Ring Road.

Indicator Layer	Study Area	Standard Value (%)	Standard Basis	Normalized Values	Evaluation Rating
Landscape fragmentation, C4	2 rings	1	Maximum value of the indicator	0.27	IV
	2–3 rings			0.31	IV
	3–4 rings			0.34	IV
	4–5 rings			0.52	III
	5 rings			0.41	III
Landscape aggregation, C5	2 rings	100	Maximum value of the indicator	0.88	I
	2–3 rings			0.88	I
	3–4 rings			0.89	I
	4–5 rings			0.92	I
	5 rings			0.91	I
Landscape diversity, C6	2 rings	1	Maximum value of the indicator	0.04	V
	2–3 rings			0.06	V
	3–4 rings			0.11	V
	4–5 rings			0.32	IV
	5 rings			0.24	IV

3.3.2. Landscape Pattern

The overall score for the landscape pattern of green space within the study area was 0.52, which corresponds to a comprehensive evaluation classification of grade III (Figure 5b). Among them, the comprehensive evaluation result of the four–five-ring landscape pattern was the highest, at 0.58, and the comprehensive evaluation grade was III. The comprehensive evaluation result in the second ring was the lowest, at 0.40 and at grade IV. The landscape pattern structure in the study area was average, and the landscape pattern structure in the Second Ring Road was not reasonable. The overall landscape fragmentation degree was serious, and landscape diversity was lacking, particularly in the area within the Second Ring Road.

Regions characterized by significant fragmentation are predominantly located within the vicinity of the Fourth Ring Road and the southeastern section of the Fifth Ring Road. The fragmentation of green spaces in other areas is high, with the exception of the zone encompassing the park (Figure 7a,b). Nevertheless, the density of grassland patches is considerably greater than that of irrigation patches within the same region, whereas the average area of grassland patches is notably smaller than that of irrigation patches (Figure 8a,b). From the perspective of different ring belts, the fragmentation degree of different green space types among each ring follows the same trend, and the fragmentation degree of irrigation and grassland in the second ring is higher. The study area shows a lack of connectivity between green spaces, except for the well-connected large parks (Figure 7c). Most of the areas with high concentrations of green space in the Fifth Ring Road belong to the distribution range of large parks in Beijing, whereas the concentration of green space in the central urban area is low (Figure 7d). The eastern and southwestern regions surrounding the Fourth and Fifth Ring Road exhibit a high and dispersed diversity of green spaces, whereas the central urban areas demonstrate a lower level of green space diversity (Figure 7e,f). The study area exhibits a low level of green space richness, quantified at 0.44, whilst the overall uniformity of green zones is high, at 0.64 (Figure 6c).

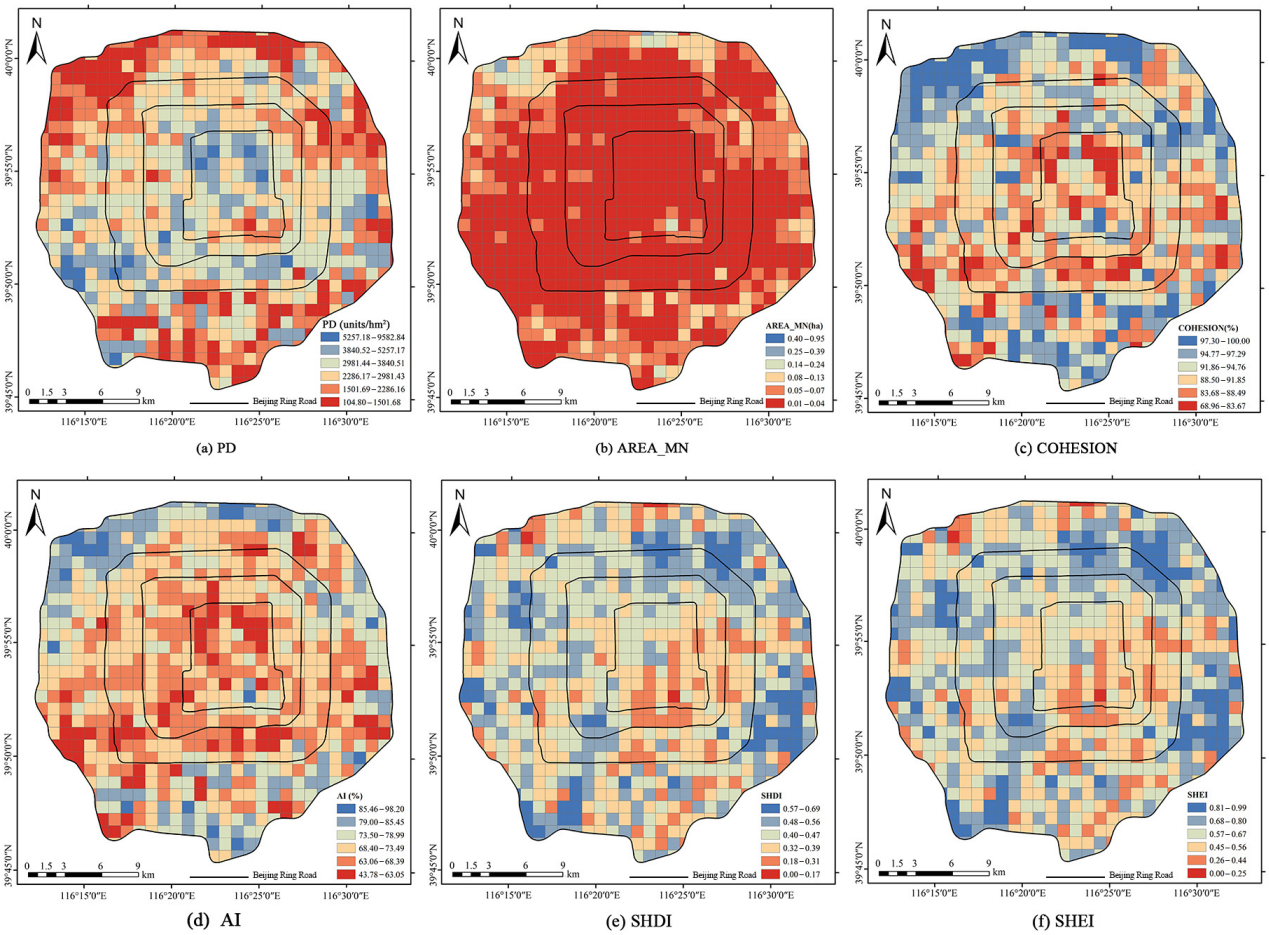


Figure 7. Landscape spatial distribution of urban green zones.

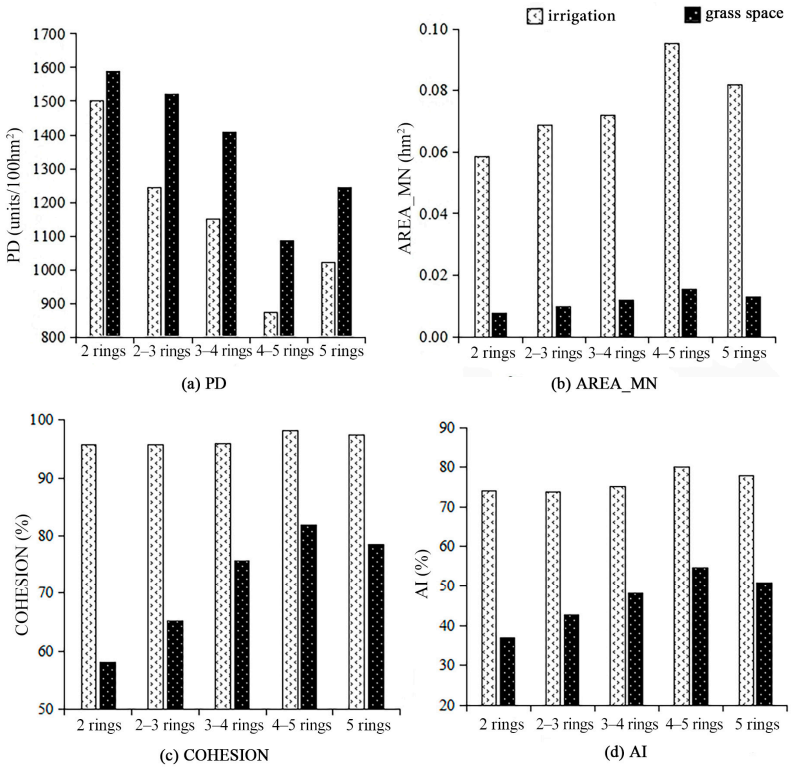


Figure 8. Column chart of urban green space landscapes.

3.4. Evaluation of the Results of Urban Green Space Service Capacity Analysis

3.4.1. Standardized Results of Urban Green Space Service Capacity

According to the requirements for urban green space service capacity in the 2022 National Garden City Selection Criteria, the required values in the selection criteria were used as standard values, and the results of various indicators were standardized. The findings from the standardization of the analysis regarding the service capability of urban green zones within the study area indicated that the accessibility of park green spaces across various zones exceeded 0.9, resulting in an evaluation classification of grade I (Table 8). Overall, the standardized coverage rate of the service radius for park green space within the study area was 0.77, resulting in an evaluation classification of grade II. In contrast, the standardized coverage rate for the service radius of park green spaces in the fourth and fifth rings was 0.81, classified as an evaluation grade of I.

Table 8. Basic quantitative characteristics of green zones.

Indicator Layer	Study Area	Standard Value (%)	Standard Basis	Normalized Values	Evaluation Rating
Coverage of the service radius of parks and green spaces C7	2 rings	85%	Selection Criteria for National Garden Cities 2022	0.75	II
	2–3 rings			0.53	III
	3–4 rings			0.62	II
	4–5 rings			0.81	I
	5 rings			0.77	II
Accessibility of parks and green spaces C8	2 rings	95%	Maximum value of the indicator	1.00	I
	2–3 rings			0.96	I
	3–4 rings			0.93	I
	4–5 rings			0.96	I
	5 rings			0.97	I

3.4.2. Evaluation of Urban Green Space Service Capacity

The overall score for the service capacity of park green spaces across the entire study area was 0.87, resulting in a comprehensive evaluation classification of grade I. Notably, the assessment of accessibility for these parks and green spaces also yielded a high score, maintaining the same evaluation grade of I. This suggests that the service capacity of urban green spaces in the study area is commendable, thereby enabling the provision of enhanced service functions to residents (Figure 5c). The overall assessment score for the service capacity of green zones within the second ring and the fourth to fifth rings exhibited the highest values, corresponding to a comprehensive evaluation classification of II. The comprehensive scores followed a descending order of the fourth to fifth rings, second ring, third to fourth rings, and second to third rings.

3.5. Comprehensive Evaluation of Green Information

The overall assessment of green zone information within the designated study area yielded a score of 0.74, categorizing it at a comprehensive evaluation level of II. This indicates that both the fundamental quantity of urban green zones and its service capacity received high scores, corresponding to a comprehensive evaluation level of I. However, notable shortcomings were brought forward in the landscape pattern of the green zones, reflected in a lower comprehensive evaluation level of III (Figure 5d). These findings indicate that the extent of green space within the fifth ring area is adequate, and the capacity for providing green space services is high. Based on different ring bands, the comprehensive evaluation results followed a descending order of the fourth–fifth rings > the third–fourth rings > within two rings > the second–third rings. Further, the fourth–fifth rings showed the highest information comprehensive evaluation results, and the comprehensive evaluation grade was II; the second–third rings showed the lowest comprehensive evaluation results at grade III.

4. Discussion

4.1. Advantages of Deep Learning Methods for Green Space Extraction

Deep learning can automatically learn the deep features of images and has achieved remarkable results in image classification. Urban green spaces exhibit an uneven distribution and significant heterogeneity. Extraction of information regarding urban green space via remote sensing technology is susceptible to interference from other terrestrial objects, which can consequently compromise extraction accuracy. In this study, both deep learning and machine learning techniques were employed to develop a classification system (U-net-SVM). First, deep learning was used to extract the information of two categories of green space and non-green space, and second, SVM was combined to further realize the classification of irrigation and grass. The final extraction results achieved an overall classification accuracy of 94.31%. Compared with a literature study [28], the overall accuracy of directly using the U-net model for the classification of irrigation and grass in Beijing urban green space was improved by 1.23%. These findings indicate that the integration of SVM with deep learning models can enhance the classification outcomes of the precision of urban green space. Further, SVM as a shallow machine learning algorithm is limited by the computational unit and cannot provide a large dataset to solve the more complex classification problems [29]. Reclassification by using the U-net framework leads to a 10.68% increase in the accuracy of green space information derived from the SVM algorithm when compared to that from the SVM alone. This increase in accuracy serves to offset the lower classification performance of SVM regarding irrigation and grass. Furthermore, it partially addresses the inherent limitations of traditional machine learning techniques, which often struggle to accurately delineate the boundaries between various categories of urban green spaces. Consequently, this approach mitigates issues related to the misclassification and omission of certain classifications, resulting in a more comprehensive representation of the edges of the extracted green space data and enhancing the overall quality of urban green space extraction outcomes [52–54]. The U-Net reduces the influence of other feature information such as building shadows, mulch, and other features to provide more accurate green space information, with better classification results [10,30]. These results indicate that the urban green zones extraction classification system (U-net-SVM) in Beijing exhibits a strong learning and generalization ability and can learn the feature information of green space from the GF-7 image, being highly feasible and accurate in refined urban green space RSI classification and extraction.

The developed classification system (U-net-SVM) for urban green space extraction in Beijing, as outlined in this study, exhibited a significant degree of accuracy during experimental evaluations. However, it is crucial to acknowledge that this study exclusively considered the spectral and texture attributes of GF-7 imagery [55]. For the labeled samples, production was only limited to the Fifth Ring Road of Beijing, which may limit the generalizability of the classification system. Consequently, future studies should investigate the integration of vegetation phenology features with elevation data to enhance the scope of sample extraction. This approach aims to further augment the generalizability of the model and its capacity for precise classification in the extraction of urban forest and grassland information.

4.2. Analysis of the Current Situation and Recommendations

Based on the findings of this study, the comprehensive index system of urban green space focuses on the urban green space, the landscape pattern, and the service function of urban green space. Compared with the Urban Landscaping Evaluation Standards, we not only extracted and classified urban green space information by using deep learning models and traditional machine learning, but also applied a combination of hierarchical analysis and an expert scoring method to comprehensively evaluate urban green space information. Within the weight values assigned to the indicator layer, the service radius coverage of urban green zones exhibited the highest value, whereas the landscape fragmentation of urban green zones exhibited the second highest one (Table 4). This result suggests that

contemporary urban green zone development should not only enhance the quality of green areas, ecological services, and social functions, but also place greater emphasis on the connectivity of urban green spaces. Among the basic quantitative characteristics, the green coverage rate is still that of the highest concern, but the proportion of blue–green space has also received significant attention. In the context of future green space development, it is imperative to not only prioritize the construction of green spaces themselves, but also consider the strategic integration of these spaces with other ecological elements within the urban environment. This approach can enhance the effective use of the ecological service value provided by urban green zones.

The findings of the present study indicate that the green zone coverage areas in the parks within the five rings of Beijing are all at a high level, and the grids with high values of tree coverage are mostly concentrated in the southern part of Dongcheng District and the western part of Chaoyang District. Trees dominate the urban green space within the five rings, influencing the size of the overall green coverage values. The standardized results of the greening coverage rate and blue–green space occupation ratio within the five rings of Beijing and different ring belts were all greater than 0.6, and the evaluation grades all reached level II or above. Among them, the standardized results for the fourth–fifth rings were the highest, and that for greening coverage was 0.82, with an evaluation grade of I. The standardized result for the blue–green space ratio was 0.81, also with grade I. The standardized values of arbor irrigation coverage within the Fifth Ring Road and different ring belts were 1, with the evaluation grade reaching I. The proportion of blue–green space within the study area exhibited a resemblance to the distribution of green coverage. In this context, the allocation of parks significantly influences the overall ratio of blue–green space within the area.

The overall assessment value of urban green zone information within the study area was 0.74, corresponding to a comprehensive evaluation classification of II. The analysis indicated that the green space within the fifth ring area is adequate, with a commendable level of service capacity and a well-structured landscape. However, several deficiencies persist. First, there is a notable lack of diversity in the region's green spaces, as evidenced by a diversity index of 0.44. Second, the fragmentation of green spaces within central urban areas is apparent. Third, the connectivity between green space patches is suboptimal, as reflected by a connectivity index of 0.64. Fourth, there is a service blind spot for park green spaces in the southeastern section of the fifth ring. These issues hinder the effective realization of the ecological functions and values associated with urban green spaces.

To enhance the ecological functionality of green spaces, development of a green space system that aligns with the requirements of social development is essential, based on the principles of landscape ecology pertaining to green spaces. It is advisable to improve biodiversity conservation within urban green spaces by expanding the area designated for grass planting while also establishing a balanced arrangement of irrigation to alleviate the status quo of the small proportion of grass coverage in the study area and its scattered distribution. Simultaneously, the construction of green corridors can enhance the connectivity of the network structure. Through scientific and reasonable development planning and an effective ecological design, the structure of urban green zones can be made complete, effectively solving the problem of poor green space connectivity. The green landscape within the fifth ring road shows a trend of gradual fragmentation from the inner to the outer area, and the connectivity of the network structure can be enhanced by expanding the width of the belt green space, strengthening road greening, and constructing corridors to connect the core green space. Emphasis should be placed on building a connection between green space patches and corridors (e.g., road green belts) to enhance the area between various green spaces; avoid the formation of small, mixed, and chaotic green zones patterns; and reduce the fragmentation [24]. This contributes to the development of esthetically pleasing landscapes, diverse ecological layers, and a stable structure within biological communities. In addressing the deficiency of green space services, in particular, in the southeastern region of the Fifth Ring Road, it is advisable to augment the quantity of

"pocket parks" and other small green areas. Moreover, it is essential to strategically use the available vacant land within the urban environment to expand the overall green space. This approach not only increases the area designated for greenery, but also improves the carbon sequestration potential of urban green spaces.

5. Conclusions

This study focused on the urban green spaces located within the Fifth Ring Road of Beijing. Deep learning technology can be a feasible approach for information extraction and classification of urban green space. Herein, the characteristics of these green spaces were examined through three distinct dimensions: the fundamental quantitative attributes of urban green zones, the landscape configuration of park green areas, and the service capacity provided by these park green spaces. The conclusions are as follows: (1) Compared with the results of only SVM extraction, the edge of green space information extracted by using the deep learning U-net model developed in this study is more complete and can effectively separate green and non-green spaces in the city, reduce the influence of other feature information on the classification results, and improve the classification accuracy by 10.68%. (2) The service capacity of green zones is of greater significance than the landscape configuration and fundamental quantitative attributes of these areas. This suggests that in the development of urban green zones in China, an increasing emphasis has been placed on the service capacity of such spaces, followed by considerations of their landscape patterns, whilst the relevance of conventional quantitative metrics is progressively diminishing. (3) The extent of green spaces within the study area is deemed adequate. The overall evaluation classification grade is II. The service capacity level of green spaces is good, the landscape structure of green spaces is reasonable, and the evaluation grade is I. The comprehensive score of overall green space construction is 0.52, and the comprehensive evaluation grade is III, indicating the occurrence of serious landscape fragmentation and lack of landscape diversity.

Supplementary Materials: The following supporting information can be downloaded at: https://www.mdpi.com/article/10.3390/rs16213946/s1, Schedule S1: Field questionnaire; Schedule S2: Statistical table of quasi-test layer; Schedule S3: Index layer score statistics table.

Author Contributions: Conceptualization, B.L. and X.X.; data curation, B.L. and X.X.; funding acquisition, B.L., X.X. and S.L. (Shaowei Lu); project administration, X.X., X.L. and S.L. (Shaoning Li); supervision, B.L.; writing—original draft, H.W., Y.D., H.L. and C.L.; writing—review and editing, B.L., X.X., N.Z., S.L. (Shaoning Li) and S.L. (Shaowei Lu). All authors have read and agreed to the published version of the manuscript.

Funding: This research was funded by Director's Foundation of Institute of Forestry and Pomology in Beijing Academy of Agriculture and Forestry Sciences (Grant No. LGSSZJJ202302), and Innovation Capacity Building of Beijing Academy of Agriculture and Forestry (Grant Nos. KJCX20230306 and KJCX20240701).

Data Availability Statement: The original contributions presented in the study are included in the article/Supplementary Material, further inquiries can be directed to the corresponding author.

Acknowledgments: The authors greatly acknowledge the support from the following units: Institute of Forestry and Pomology, Beijing of Agriculture and Forestry Sciences; Beijing Yanshan Forest Ecosystem Observation and Research Station; and Forestry College of Shenyang Agricultural University.

Conflicts of Interest: The authors declare no conflicts of interest.

References

1. Lin, L.; Yan, J.; Ma, K.; Zhou, W.; Chen, G.; Tang, R.; Zhang, Y. Characterization of particulate matter deposited on urban tree foliage: A landscape analysis approach. *Atmos. Environ.* **2017**, *171*, 59–69. [CrossRef]
2. Yan, J.L.; Lin, L.; Zhou, W.; Han, L.; Ma, K. Quantifying the characteristics of particulate matters captured by urban plants using an automatic approach. *J. Environ. Sci.* **2016**, *39*, 259–267. [CrossRef]
3. Zhang, L.; Peng, J.; Liu, Y.; Wu, J. Coupling ecosystem services supply and human ecological demand to identify landscape ecological security pattern: A case study in Beijing–Tianjin–Hebei region, China. *Urban Ecosyst.* **2017**, *20*, 701–714. [CrossRef]

4. Adams, M.P.; Smith, P.L. A systematic approach to model the influence of the type and density of vegetation cover on urban heat using remote sensing. *Landsc. Urban Plan.* **2014**, *132*, 47–54. [CrossRef]
5. Jenerette, G.D.; Harlan, S.L.; Buyantuev, A.; Stefanov, W.L.; Declet-Barreto, J.; Ruddell, B.L.; Myint, S.W.; Kaplan, S.; Li, X. Micro-scale urban surface temperatures are related to land-cover features and residential heat related health impacts in Phoenix, AZ USA. *Landsc. Ecol.* **2016**, *31*, 745–760. [CrossRef]
6. Thompson, C.W.; Roe, J.; Aspinall, P.; Mitchell, R.; Clow, A.; Miller, D. More green space is linked to less stress in deprived communities: Evidence from salivary cortisol patterns. *Landsc. Urban Plan.* **2012**, *105*, 221–229. [CrossRef]
7. *GB/T50563-2010*; Evaluation Standard for Urban Landscaping and Greening. Ministry of Housing and Urban-Rural Development: Beijing, China, 2010.
8. Hammou, B.A.; Lahcen, A.A.; Mouline, S. Towards a real-time processing framework based on improved distributed recurrent neural network variants with fastText for social big data analytics. *Inf. Process Manag.* **2020**, *57*, 102122. [CrossRef]
9. Li, Y.; Yang, Y.; Yan, X.; Li, Y. Engineering Applications of Urban Green Space Planning in Mountainous Areas: An Improved Structure-based RS Land Class Information Extraction Method for U-Net Networks. *Earth Sci Inform.* **2023**, *16*, 4187–4198. [CrossRef]
10. Jiao, Y.; Wang, X.; Wang, W.; Li, S. Image Semantic Segmentation Fusion of Edge Detection and AFF Attention Mechanism. *Appl. Sci.* **2022**, *12*, 11248. [CrossRef]
11. Rui, L.; Buccolieri, R.; Gao, Z.; Ding, W.; Shen, J. The Impact of Green Space Layouts on Microclimate and Air Quality in Residential Districts of Nanjing, China. *Forests* **2018**, *9*, 224. [CrossRef]
12. Chen, C.; Chen, H.; Liang, J.; Huang, W.; Xu, W.; Li, B.; Wang, J. Extraction of Water Body Information from Remote Sensing Imagery While Considering Greenness and Wetness Based on Tasseled Cap Transformation. *Remote Sens.* **2022**, *14*, 3001. [CrossRef]
13. Hamaguchi, R.; Hikosaka, S. Building Detection from Satellite Imagery using Ensemble of Size-Specific Detectors. In Proceedings of the 2018 IEEE/CVF Conference on Computer Vision and Pattern Recognition Workshops (CVPRW), Salt Lake City, UT, USA, 18–22 June 2018; pp. 18–22.
14. Zhao, H.; Guan, Y. Multi-feature-marks Based Information Extraction of Urban Green Space Along Road. *Int. Arch. Photogramm. Remote Sens. Spat. Inf. Sci.* **2018**, *XLII-3*, 2353–2357. [CrossRef]
15. Liu, H.; Luo, J.; Huang, B.; Hu, X.; Sun, Y.; Yang, Y.; Xu, N.; Zhou, N. DE-Net: Deep Encoding Network for Building Extraction from High-Resolution Remote Sensing Imagery. *Remote Sens.* **2019**, *11*, 2380. [CrossRef]
16. Neema, M.N.; Ohgai, A. Multitype Green-Space Modeling for Urban Planning Using GA and GIS. *Environ. Plan B Plan. Des.* **2013**, *40*, 447–473. [CrossRef]
17. Zhao, K.; Kang, J.; Jung, J.; Sohn, G. Building Extraction from Satellite Images Using Mask R-CNN with Building Boundary Regularization. In Proceedings of the 2018 IEEE/CVF Conference on Computer Vision and Pattern Recognition Workshops (CVPRW), Salt Lake City, UT, USA, 18–22 June 2018; pp. 18–22.
18. Helber, P.; Bischke, B.; Dengel, A.; Borth, D. Euro SAT: A Novel Dataset and Deep Learning Benchmark for Land Use and Land Cover Classification. *IEEE J. Sel. Top. Appl. Earth Obs. Remote Sens.* **2019**, *12*, 2217–2226. [CrossRef]
19. Vigneshwaran, S.; Vasantha, K.S. Comparison of classification methods for urban green space extraction using very high resolution worldview-3 imagery. *Geocarto Int.* **2019**, *36*, 1–14. [CrossRef]
20. Martins, G.B.; La Rosa, L.E.C.; Happ, P.N.; Coelho Filho, L.C.T.; Santos, C.J.F.; Feitosa, R.Q.; Ferreira, M.P. Deep learning-based tree species mapping in a highly diverse tropical urban setting. *Urban For. Urban Green.* **2021**, *64*, 127241. [CrossRef]
21. Zhang, Z.; Wang, Y.; Zhu, D. Overheating in the Tree Shade of Urban Parks: A Field Study of Thermal Adaption in China. *Atmosphere* **2024**, *15*, 575. [CrossRef]
22. Hlusko, R.; Stanek, R.; Ďurcek, P.; Kusendová, D. Urban public transport system accessibility for different groups of residents: Case of Bratislava city. *Case Stud. Transp. Policy* **2024**, *16*, 101200. [CrossRef]
23. Bhor, N.; Mayavel, D. A study on analysing sociospatial distribution and equity in access to urban parks in Bengaluru, India. *Lancet Planet. Health* **2024**, *8*, S13. [CrossRef]
24. Sun, P.; Liu, P.; Song, Y. Seasonal variations in urban park characteristics and visitation patterns in Atlanta: A big data study using smartphone user mobility. *Urban For. Urban Green.* **2024**, *91*, 128166. [CrossRef]
25. Fasihi, H.; Parizadi, T. Analysis of spatial equity and access to urban parks in Ilam, Iran. *J. Environ. Manag.* **2020**, *260*, 110–122. [CrossRef] [PubMed]
26. Luo, S.; Xie, J.; Furuya, K. Assessing the preference and restorative potential of urban park blue space. *Land* **2021**, *10*, 1233. [CrossRef]
27. Zhang, J.; Shen, H. Geo-spatial analysis and optimization strategy of park green space landscape pattern of Garden City–A case study of the central district of Mianyang City Sichuan Province. *Eur. J. Remote Sens.* **2020**, *53*, 309–315.
28. Li, F.X.; Song, K.L.; Feng, X.G.; Li, M. Research on the functional value of green space in Xi'an Urban Park. *J. Xi'an Univ. Archit. Technol. Nat. Sci. Ed.* **2023**, *55*, 783–790.
29. Mohammed Abdul Athick, A.S.; Shankar, K. Data on land use and land cover changes in Adama Wereda, Ethiopia, on ETM+, TM and OLI-TIRS landsat sensor using PCC and CDM techniques. *Data Brief* **2019**, *24*, 103880. [CrossRef]
30. Xing, W.; Liu, J.R.; Xu, S.X. Extraction and analysis of urban green space in the main urban area of Guangzhou based on TM images. *Mapp. Spat. Geogr. Inf.* **2020**, *43*, 123–125.

31. Chen, X.; Wang, Y. Extract Method of Urban Greenbelt Based on TM Image. *Adv. Mater. Res.* **2013**, *610*, 3562–3565. [CrossRef]
32. Zhao, L.L.; Zhao, Y.S.; Zhang, J.H.; Dong, G.H. A study on methods of obtaining greenland information based on ETM+ in Shenzhen. *Remote Sens. Technol. Appl.* **2005**, *6*, 596–600.
33. Sarı, E.N.; Bayraktar, S. The role of park size on ecosystem services in urban environment: A review. *Environ. Monit. Assess.* **2023**, *195*, 1072. [CrossRef]
34. Griffith, J.A.; Martinko, E.A.; Price, K.P. Landscape structure analysis of Kansas at three scales. *Landsc. Urban Plan.* **2000**, *52*, 45–61. [CrossRef]
35. Ronneberger, O.; Fischer, P.; Brox, T. U-Net: Convolutional Networks for Biomedical Image Segmentation. In Proceedings of the Medical Image Computing and Computer-Assisted Intervention—MICCAI 2015, Munich, Germany, 5–9 October 2015.
36. Wickham, J.D.; Riitters, K.H.; Wade, T.G.; Vogt, P. A national assessment of green infrastructure and change for the conterminous United States using morphological image processing. *Landsc. Urban Plan.* **2010**, *94*, 186–195. [CrossRef]
37. Lu, D.; Mao, W.; Yang, D.; Zhao, J.; Xu, J. Effects of land use and landscape pattern on PM2.5 in Yangtze River Delta, China. *Atmos. Pollut. Res.* **2018**, *9*, 705–713. [CrossRef]
38. Yang, Y.; Sun, W.; Su, G. A Novel Support-Vector-Machine-Based Grasshopper Optimization Algorithm for Structural Reliability Analysis. *Buildings* **2022**, *12*, 855. [CrossRef]
39. Li, Z.; Wang, Z.; Liu, X.; Sun, S.; Ma, X.; Zuo, Y. Using random forest and improved CA-Markov model to evaluate the effect of *Spartina alterniflora* clearing on wetland use and landscape pattern in the Yellow River Delta wetland. *Acta Ecol. Sin.* **2024**, *44*, 8366–8382.
40. Xu, Z.; Zhou, Y.; Wang, S.; Wang, L.; Li, F.; Wang, S.; Wang, Z. A Novel Intelligent Classification Method for Urban Green Space Based on High-Resolution Remote Sensing Images. *Remote Sens.* **2020**, *12*, 3845. [CrossRef]
41. Wang, H.; Li, G.; Wang, Z. Fast SVM classifier for large-scale classification problems. *Inf. Sci.* **2023**, *642*, 119136. [CrossRef]
42. Myeong, S.; Nowak, D.J.; Duggin, M.J. A temporal analysis of urban forest carbon storage using remote sensing. *Remote Sens. Environ.* **2006**, *101*, 277–282. [CrossRef]
43. Kussul, N.; Lavreniuk, M.; Skakun, S.; Shelestov, A. Deep Learning Classification of Land Cover and Crop Types Using Remote Sensing Data. *IEEE Geosci. Remote Sens. Lett.* **2017**, *14*, 778–782. [CrossRef]
44. Wu, J.G. Landscape sustainability science: Ecosystem services and human well-being in changing landscapes. *Landsc. Ecol.* **2013**, *28*, 999–1023. [CrossRef]
45. Neyns, R.; Canters, F. Mapping of Urban Vegetation with High-Resolution Remote Sensing: A Review. *Remote Sens.* **2022**, *14*, 1031. [CrossRef]
46. Ghosh, A.; Ehrlich, M.; Shah, S.; Davis, L.; Chellappa, R. Stacked U-Nets for Ground Material Segmentation in Remote Sensing Imagery. In Proceedings of the 2018 IEEE/CVF Conference on Computer Vision and Pattern Recognition Workshops (CVPRW), Salt Lake City, UT, USA, 18–22 June 2018; pp. 257–261.
47. Gong, F.; Zheng, Z.C.; Ng, E. Modeling Elderly Accessibility to Urban Green Space in High Density Cities: A Case Study of Hong Kong. *Procedia Environ. Sci.* **2016**, *36*, 90–97. [CrossRef]
48. Huang, Y.Y.; Lin, T.; Zhang, G.Q. Spatiotemporal patterns and inequity of urban green space accessibility and its relationship with urban spatial expansion in China during rapid urbanization period. *Sci. Total Environ.* **2021**, *809*, 151123. [CrossRef] [PubMed]
49. Qian, Y.G.; Zhou, W.Q.; Li, W.F.; Han, L.J. Understanding the dynamic of greenspace in the urbanized area of Beijing based on high resolution satellite images. *Urban For. Urban Green.* **2015**, *14*, 39–47. [CrossRef]
50. Daniele, R.L. Accessibility to greenspaces: GIS based indicators for sustainable planning in adense urban context. *Ecol. Indic.* **2014**, *42*, 122–134.
51. Yuan, Y.N.; Jin, Y.F.; Nie, X.J.; Ling, R.; Wu, S.S.; Lan, S. Study on the dynamics of Shanghai urban landscape pattern index based on Fragstats4. *J. Shandong Agric. Univ. Nat. Sci. Ed.* **2020**, *51*, 1157–1162.
52. Zhang, B.; Yang, X.M.; Gao, L.R.; Meng, Y.; Sun, X.; Xiao, C.C.; Ni, L. Geographical cognitive model and method for intelligent interpretation of remote sensing big data. *Acta Geod. Cartogr. Sin.* **2022**, *51*, 1398–1415.
53. Zhang, Y.J.; Fan, C.; Huang, K.; Liu, Y.; Zu, J.; Zhu, J. Opportunities and challenges for the application of remote sensing in ecosystem ecology. *J. Ecol.* **2017**, *36*, 809–823.
54. Zhou, Y.D.; Zhou, Z.D. Forest landscape pattern of Hainan Island based on GIS and Fragstats. *J. Cent. South Univ. For. Technol.* **2015**, *35*, 78–83.
55. Xi, J.L.; Wu, Z.F.; Zhang, H.; Wei, J.Y. Comprehensive evaluation of green space service capacity in central urban parks: Model and case. *J. Ecol. Environ.* **2020**, *29*, 1044–1053.

Disclaimer/Publisher's Note: The statements, opinions and data contained in all publications are solely those of the individual author(s) and contributor(s) and not of MDPI and/or the editor(s). MDPI and/or the editor(s) disclaim responsibility for any injury to people or property resulting from any ideas, methods, instructions or products referred to in the content.